Mon. Not. R. Astron. Soc. 000, 000–000 (0000) Printed 24 February 2000 (MN LaTeX style file v1.4)

What Damped Ly-alpha Systems Tell Us About the Radial Distribution of Cold Gas at High Redshift

Ariyeh H. Maller[1,2], Jason X. Prochaska[3], Rachel S. Somerville[2,4] and Joel R. Primack[1]
[1] *Physics Department, University of California, Santa Cruz, CA 95064*
[2] *Racah Institute for Physics, The Hebrew University, Jerusalem, ISRAEL, 91904*
[3] *Observatories of the Carnegie Institution of Washington, Pasadena CA 91101*
[4] *Institute of Astronomy, Cambridge University, Cambridge, CB3 0HA, UK*

24 February 2000

ABSTRACT
We investigate the properties of damped Lyman-α systems (DLAS) in semi-analytic models, focusing on whether the models can reproduce the kinematic properties of low-ionization metal lines described by Prochaska & Wolfe (1997b, 1998). We explore a variety of approaches for modelling the radial distribution of the cold neutral gas associated with the galaxies in our models, and find that our results are very sensitive to this ingredient. If we use an approach based on Fall & Efstathiou (1980), in which the sizes of the discs are determined by conservation of angular momentum, we find that the majority of the DLAS correspond to a single galactic disc. These models generically fail to reproduce the observed distribution of velocity widths. In alternative models in which the gas discs are considerably more extended, a significant fraction of DLAS arise from lines of sight intersecting multiple gas discs in a common halo. These models produce kinematics that fit the observational data, and also seem to agree well with the results of recent hydrodynamical simulations. Thus we conclude that Cold Dark Matter based models of galaxy formation can be reconciled with the kinematic data, but only at the expense of the standard assumption that DLAS are produced by rotationally supported gas discs whose sizes are determined by conservation of angular momentum. We suggest that the distribution of cold gas at high redshift may be dominated by another process, such as tidal streaming due to mergers.

Key words: quasars:absorption lines–galaxies:formation–galaxies:spiral

1 INTRODUCTION

This paper is the first in a series of papers that examines the properties of Damped Lyman-α Systems (DLAS) in the context of Cold Dark Matter (CDM) based Semi-Analytic Models (SAMs). Traditionally, DLAS are believed to be the progenitors of present day spiral galaxies (Wolfe 1995) and thus any model of galaxy formation must also account for their properties. The current wealth of observational data on DLAS includes their number density, column density distribution, metallicities, and kinematic properties — see Lanzetta, Wolfe & Turnshek (1995); Storrie-Lombardi, Irwin, & MCMahon (1996); Storrie-Lombardi & Wolfe (2000); Pettini et al. (1994); Lu et al. (1996); Pettini et al. (1997); Prochaska & Wolfe (1997b, 1998, 1999, 2000); Wolfe & Prochaska (2000). These data potentially provide important constraints on cosmology and theories of galaxy formation. Here we especially focus on the new kinematic data.

Previously, the number density of DLAS has been used to provide constraints on cosmological models (Mo & Miralda-Escude 1994; Kauffmann & Charlot 1994; Ma & Bertschinger 1994; Klypin et al. 1995). These studies assumed a simple correspondance between collapsed dark matter halos and cold gas to obtain upper limits on the amount of cold gas that could be present. Gas cooling, star formation, supernovae feedback, and ionization were neglected. A different approach was used by Lanzetta et al. (1995); Wolfe et al. (1995); Pei & Fall (1995); Pei, Fall & Hauser (1999), in which the observed metallicities and *observed* number densities of the DLAS were used to model global star formation and chemical enrichment in a self-consistent way. The latter approach was set in a classical "closed-box" style framework rather than a cosmological context.

Clearly, in order to model DLAS realistically one needs to include the astrophysical processes of gas dynamics and cooling, star formation, and chemical enrichment within a cosmological framework. However, this is a challenge with our current theoretical and numerical capability. Cosmological N-body simulations with hydrodynamics are hampered by the usual limitations of volume and resolution. This is apparent in, for example, the recent work by Gardner et al. (1999), in which it was found that even rather high-resolution hydrodynamical simulations could not account for most of the observed DLAS. Gardner et al. (1999) concluded that the majority of the damped Ly-α absorption must arise from structures below the resolution of their simulations. In addition, it is well known that such simulations fail to reproduce the sizes and angular momenta of present day observed spiral galaxies (Steinmetz 1999). One might therefore be suspicious of the accuracy of their representation of the spatial distribution of the cold gas that gives rise to DLAS at high redshift. Because observational samples of DLAS are cross-section weighted, these properties are likely to introduce crucial selection effects. Semi-analytic approaches can deal with nearly arbitrary resolution and volumes, but are limited in the sophistication and accuracy of their physical "recipes". In particular, most previous SAMs have focussed on the bulk properties of galaxies, and have not attempted to model the spatial location of galaxies relative to one another or the spatial distribution of gas and stars within galaxies.

The only previous attempt to model the properties of DLAS in a CDM framework is the work of Kauffmann (1996) (hereafter K96). In K96 the radial distribution of cold gas in galactic discs was modelled by assuming that the initial angular momentum of the gas matched that of the halo, and that angular momentum was conserved during the collapse. Star formation was then modelled using the empirical law of Kennicutt (1989, 1998), in which the star formation is a function of the surface density of the gas, and cuts off below a critical threshold density. K96 then showed that the number density, column density distribution, and metallicities of observed DLAS could be reasonably well reproduced within the Standard Cold Dark Matter (SCDM) cosmology, and predicted the distribution of circular velocities of discs that would give rise to DLAS. Assuming that each observed DLAS corresponds to a single galactic disc, this can then be compared with the observed distribution of velocity widths derived from the kinematics of unsaturated, low-ionization metal lines (Prochaska & Wolfe 1997b, 1998).

Prochaska & Wolfe found the velocity distribution predicted by K96 to be strongly inconsistent with their data. Furthermore Jedamzik & Prochaska (1998) showed that the thick rotating disc model favored by Prochaska & Wolfe (1997b) could only be reconciled with a finely tuned CDM model. But CDM actually predicts that halos will have much substructure, and Haehnelt, Steinmetz & Rauch (1998) found that large Δv velocity profiles consistent with those observed by Prochaska & Wolfe are produced in their very high-resolution hydrodynamical simulations. These profiles arose not from the rotation of a single disc, but from lines of sight intersecting multiple proto-galactic "clumps". Subsequently, McDonald & Miralda-Escudé (1999) also showed with a simple analytical model that DLAS produced by intersection with a few gas clouds could create kinematics consistent with the observations in a CDM universe.

These results were encouraging but remain somewhat inconclusive. The hydro simulations do not allow the construction of a statistical, cross-section selected sample of DLAS, so it is difficult to assess how typical are the systems that they identified. In addition, these simulations were restricted to a single cosmology (SCDM), and did not include star formation or supernovae feedback. The generic difficulty of hydro simulations in producing reasonable discs at low redshift has already been noted. Therefore a further investigation using detailed semi-analytic models is worthwhile.

In the standard CDM picture of galaxy formation (based on White & Rees 1978; Blumenthal et al. 1984) gas is heated to the virial temperature when a halo forms and then cools and falls into the centre of the halo where it subsequently forms stars. In SAMs, which include the hierarchical formation of structure, this process happens numerous times as halos continually merge and form larger structures. This naturally results in halos that may contain many gaseous discs, each one associated with a sub-halo that prior to merging had been an independent halo. In this paper, we explore the possibility that such a scenario can account for the observed kinematics of the DLAS in a manner analogous to the proto-galactic clumps of Haehnelt et al. (1998) and the gas clouds of McDonald & Miralda-Escudé (1999). Here, however, the number densities, gas contents, and metallicities of these proto-galaxies are determined by the full machinery of the SAMs, which have been tuned to produce good agreement with the optical properties of galaxies at low and high redshift. We introduce new ingredients to describe the kinematics of satellite galaxies within dark matter halos, and the spatial distribution of cold gas in discs. We also include a model that is not based on the machinery of the SAMs to demonstrate that our general conclusions are not overly dependent on the specifics of how these processes are handled in the SAMs.

We start with a review of the the observational properties of DLAS (section 2). Next, section 3 gives a brief description of the ingredients of the SAMs, and describes how we simulate the observational selection process for DLAS and produce simulated velocity profiles. We demonstrate in section 4.1 that gaseous discs with sizes determined by conservation of angular momentum fail to match the kinematic data, and then in section 4.2 show that acceptable solutions can be found if the gaseous discs have a large radial extent. Section 5 examines the sensitivity of our results to a number of model parameters. In section 6 we discuss the properties of the gas discs in our model and compare them to HI observations of local spirals and with the results of hydro simulations. Lastly we close with some discussion and conclusions.

2 OBSERVATIONAL PROPERTIES OF DLAS

DLAS are defined as those absorption systems that have a column density of neutral hydrogen in excess of 2×10^{20} atoms per square centimeter (Wolfe et al. 1986). Prochaska & Wolfe (1996, 1997a) found that the velocity profiles of low ionization state metal lines (Si^+, Fe^+, Cr^+, etc.) trace each other well and therefore presumably the kinematics of the cold gas.

They therefore undertook to obtain a large sample of the kinematic properties of DLAS as measured by the associated metal lines and compared them to the predictions from a number of models. All of the observations were obtained with HIRES (Vogt 1992) on the 10m Keck I telescope.

None of the DLAS were chosen with *a priori* kinematic information and the metal line profiles were selected according to strict criteria including that they not be saturated, therefore it is believed that the sample is kinematically unbiased. We have taken care that our model profiles match the resolution and signal-to-noise of the observations and that they conform to the same profile selection criteria.

Prochaska & Wolfe (1997b, hereafter PW97) developed four statistics to characterize the velocity profiles of the gas, which we also use to compare our models to the data set of 36 velocity profiles in Prochaska & Wolfe (1998) and Wolfe & Prochaska (2000). The four statistics as defined in PW97 are:

- Δv, the velocity interval statistic, defined as the width containing 90% of the optical depth.
- f_{mm}, the mean-median statistic, defined as the distance between the mean and the median of the optical depth profile, divided by $\Delta v/2$.
- f_{edg}, the edge-leading statistic, defined as the distance between the highest peak and the mean, divided by $\Delta v/2$.
- f_{2pk}, the two-peak statistic, defined as the distance of the second peak to the mean. Positive if on the same side of the mean as the first peak and negative otherwise.

The other observational data that our modeling of DLAS must conform to are the differential density distribution $f(N)$ (the number of absorbers per unit column density per unit absorption distance) and the distribution of metal abundances. The most recent determination of $f(N)$ comes from Storrie-Lombardi & Wolfe (2000). The metal abundances in damped systems at high redshift ($z > 2$) have most recently been compiled by Pettini et al. (1997) and Prochaska & Wolfe (1999, 2000).

3 MODELS

3.1 Semi-Analytic Models

We use the semi-analytic models developed by the Santa Cruz group (Somerville 1997; Somerville & Primack 1999; Somerville, Primack & Faber 2000), which are based on the general approach pioneered by White & Frenk (1991), Kauffmann, White & Guiderdoni (1993) and Cole et al. (1994). Our analysis is based on the fiducial ΛCDM model presented in Somerville et al. (2000, hereafter SPF), which was shown there to produce good agreement with many properties of the observed population of Lyman-break galaxies at redshift $\sim 2.5 - 4$, and the global evolution with redshift of the star formation density, metallicity, and cold gas density of the Universe. Below we describe the aspects of the SAMs most relevant to modeling the DLAS, and refer the reader to SPF and Somerville & Primack (1999, hereafter SP), for further details.

3.1.1 halos and sub-halos

The number density of virialized dark matter halos as a function of mass and redshift is given by an improved Press-Schechter model (Sheth & Tormen 1999). The merging history of each dark matter halo at a desired output redshift is then determined according to the prescription of Somerville & Kolatt (1999). As in SP, we assume that halos with velocity dispersions less than $\sim 30\,\mathrm{km\,s^{-1}}$ are photoionized and that the gas within them cannot cool or form stars. This sets the effective mass resolution of our merger trees. When halos merge, the central galaxy in the largest progenitor halo becomes the new central galaxy and all other halos become "sub-halos". These sub-halos are placed at a distance $f_{mrg} r_{\rm vir}$ from the centre of the new halo, where $r_{\rm vir}$ is the virial radius of the new halo. We will take f_{mrg} to be 0.5 as in SP, but will examine the importance of this parameter in section 5.

After each merger event, the satellite galaxies fall towards the centre of the halo due to dynamical friction. We calculate the radial position of each satellite within the halo using the differential formula

$$r_{fric}\frac{dr_{fric}}{dt} = -0.42\epsilon^{0.78}\frac{Gm_{sat}}{V_c}\ln{(1+\frac{m_h}{m_{sat}})}. \qquad (1)$$

Here m_h and m_{sat} are the masses of the halo and satellite respectively, and ϵ is a "circularity" parameter which describes the orbit of the satellite and is drawn from a flat distribution between 0.02 and 1 as suggested by N-body simulations (Navarro, Frenk & White 1995). The halos are assumed to have a singular isothermal density profile and to be tidally truncated where the density of the sub-halo is equal to that of its host at its current radius. When a sub-halo reaches the centre of the host, it is destroyed and the galaxy contained within it is merged with the central galaxy.

3.1.2 gas and stars

In our models, gas can occupy one of two phases, cold or hot. Halos contain hot gas, which is assumed to be shock-heated to the virial temperature of the halo and distributed like the dark matter in a singular isothermal sphere (SIS). After a cooling time $t = t_{\rm cool}$ has elapsed, gas at a sufficiently high density (corresponding to the gas within the "cooling radius" r_{cool}) is assumed to cool and condense into a disc. This cold gas then becomes available for star formation.

Star formation takes place in both a quiescent and bursting mode. Quiescent star formation proceeds in all discs whenever gas is present, according to the expression

$$\dot{m}_* = \frac{m_{cold}}{\tau_*}, \qquad (2)$$

where m_{cold} is the mass in cold gas and τ_* is an efficiency factor that is fixed using nearby galaxy properties (see below). In the bursting mode, which takes place following galaxy-galaxy mergers, the efficiency of star formation is sharply increased for a short amount of time ($\sim$ 50–100 Myr). The efficiency and timescale of the starbursts has been calibrated using the results of hydrodynamical simulations as described in SPF. The merger rate is determined by the infall of satellites onto the central galaxy, as described above, and the collision of satellites with one another according to a modified mean-free path model (see SP and SPF).

In association with star formation, supernovae may reheat and expell the cold gas from the disc and/or the halo. We model this using the disc-halo model of SP, in which the efficiency of the feedback is larger for galaxies residing in smaller potential wells. These stars also produce metals, which are mixed with the cold inter-stellar gas, and may be subsequently ejected and mixed with the hot halo gas, or ejected into the diffuse extra-halo IGM. Our simple constant-yield, instantaneous recycling model for chemical enrichment produces reasonable agreement with observations of metallicities of nearby galaxies (SP), the redshift evolution of the metallicity of cold gas implied by observations of DLAS, and the metallicity of the Lyman-α forest (SPF).

The main free parameters of the model are the star formation efficiency, τ_*, the supernovae feedback efficiency ϵ^0_{SN} and the mass of metals produced per unit mass of stars, or effective yield, y. As described in SP, we set these parameters so that a "reference galaxy" with a rotation velocity of 220 $\mathrm{km\,s^{-1}}$ at redshift zero has a luminosity, cold gas mass fraction and metallicity in agreement with local observations. Good agreement is then obtained with optical and HI properties of local galaxies (SP), and optical properties of high redshift galaxies (SPF).

3.1.3 cosmology

In this paper our fiducial models are set within a ΛCDM cosmology with $\Omega_\Lambda = 0.7, \Omega_0 = 0.3, h = 0.7$, corresponding to model ΛCDM.3 in SP, and the fiducial model of SPF. We have presented similar results for a standard CDM ($\Omega_0 = 1$) cosmology in Maller et al. (1999). As recent observational results seem to favor a cosmological constant (Perlmutter et al. 1999) and a flat universe (Melchiorri et al. 1999) we feel justified in focusing on only this cosmology. In section 5 we show that our results are not very sensitive to the assumed cosmology.

We focus our analysis on halos at an output redshift of $z = 3$. We have also performed an identical analysis on halos at $z = 2$ and find no significant differences, consistent with the kinematic data and column density distribution $f(N)$, which show little evolution over this range. We expect to see evolution both in low redshift ($z < 1.5$) and very high redshift ($z > 4$) systems, however we will defer discussion of this to a future paper.

3.2 The Spatial Distribution of Cold Gas

The standard SAMs do not provide us with information on the radial distribution of gas and stars in the model galaxies. It is reasonable to assume that the surface density of the cold gas is important in determining the star formation rate in the gaseous discs, and in this case the radial distribution of gas should be modelled self-consistently within the SAMs. This has been done in the models of K96. However, there are many uncertainties attached to modelling the structure of the gaseous disc in the initial collapse, and how it may be modified by mergers, supernovae feedback, and secular evolution. Therefore here we choose a different approach. The SAMs described above produce good agreement with the observed $z \sim 3$ luminosity function of Lyman-break galaxies (SPF). The total mass density of cold gas at this redshift is also in agreement with estimates derived from observations from DLAS (Storrie-Lombardi et al. 1996; Storrie-Lombardi & Wolfe 2000). We can therefore ask how this gas must be distributed relative to these galaxies in order to produce agreement with an independent set of observations, the kinematic data.

We assume that the vertical profile of the gas is exponential, and consider two functional forms for the radial profiles of the cold gas: exponential and $1/R$ (Mestel). The exponential radial profile is motivated by observations of local spiral galaxies, which indicate that the light distribution of the disc is well fit by an exponential (Freeman 1970). If one assumes that as cold gas is converted into stars its distribution doesn't change (which many theories of disc sizes implicitly assume), then the profile of cold gas at high redshift should also be exponential. The column density of the gas may then be parameterized by two quantities, the scale length R_g and the central column density $N_0 \equiv m_{\rm gas}/(2\pi\mu m_H R_g^2)$ (where $m_{\rm gas}$ is the total mass of cold gas in the disc, m_H is the mass of the hydrogen atom and μ is the mean molecular weight of the gas, which we take to be 1.3 assuming 25% of the gas is Helium). The column density as a function of radius is given by

$$N_{exp}(R) = N_0 \exp\left[-\frac{R}{R_g}\right] \tag{3}$$

The $1/R$ profile, sometimes refered to as a Mestel distribution (Mestel 1963), is also motivated by observations. Radio observations (Bosma 1981) have shown that the surface density of HI gas is proportional to the projected surface density of the total mass, which for a perfectly flat rotation curve would imply a $1/R$ distribution. We parameterize the Mestel disc in terms of the truncation radius R_t and the column density at that radius $N_t \equiv m_{\rm gas}/(2\pi\mu m_H R_t^2)$:

$$N_{mes}(R) = N_t \frac{R_t}{R}. \tag{4}$$

In the limit of infinitely thin discs, we can calculate the cross section for these distributions analytically and use them to check our numeric code. For an exponential disc, the inclination averaged cross section is

$$\sigma(N' > N) = \frac{\pi R_g^2 \gamma_m^2}{2}(\ln^2 \frac{N_0}{N\gamma_m} + \ln \frac{N_0}{N\gamma_m} + \frac{1}{2}) \tag{5}$$

(Bartelmann & Loeb 1996). The variable $\gamma_m = \min[\frac{N_0}{N}, 1]$ is introduced because a column density of N when $N > N_0$ can only be reached if the disc is inclined such that $\cos\theta > \gamma_m$. For Mestel discs the corresponding expression is

$$\sigma(N' > N) = \pi R_t^2 \frac{N_t}{N}(\frac{1}{2} - \ln \frac{N_t}{N}) \tag{6}$$

for $N > N_t$.

3.3 Selecting and Modeling DLAS

The fiducial SPF "standard SAMs" provide us with a list of galaxies contained within a halo of a given mass or circular velocity at a given redshift. For each of these galaxies, we are also provided with the internal circular velocity, radial distance from the halo centre, stellar exponential scale length, and the cold gas, stellar, and metal content of its disc. We distribute the galaxies randomly on circular orbits (we discuss the importance of this simplification in section 5) and assign them random inclinations.

We create twenty realizations of a grid of halos with circular velocities between 50 $\mathrm{km\,s^{-1}}$ and 500 $\mathrm{km\,s^{-1}}$. These correspond to different Monte Carlo realizations of the halos' merging histories. We then choose a model for the radial distribution of the gas and calculate the surface density distribution, constrained by the total gas mass as determined by the SAMs. We create twenty random realizations of the satellite orbits and inclinations in each of the four hundred halos and calculate the column density along each line of sight. The number of lines of sight passed through each halo is determined by the cross-section weighted probability of intersecting a halo of that mass. The total number of lines of sight is chosen to produce about ten thousand DLAS. Each line of sight that passes through a total column density exceeding $2 \times 10^{20}\,\mathrm{cm}^{-2}$ is then saved (along with all the properties of the halo that it is found in) and analyzed using the methods of PW97.

To create synthesized spectra we must include substructure in the gas discs, which we do by assuming that the gas is distributed in small clouds within the disc. The necessary parameters are: σ_{int}, the internal velocity dispersion of each cloud; N_c, the number of clouds; and σ_{cc}, their isotropic random motions. Following PW97, we take $\sigma_{int} = 4.3\,\mathrm{km\,s}^{-1}$ and $N_c = 5$; both values were derived from Voigt profile fits to the observations with $N_c = 5$ being the minimum acceptable number of individual components. Increasing the cloud number, N_c to as high as 60 does not improve the goodness of fit (PW97) for a disc model like we are considering here because our model discs are relatively thin. Also we take $\sigma_{cc} = 10\,\mathrm{km\,s}^{-1}$, since we assume that the gas discs are cold. These internal velocities are in addition to the circular velocity of the disc and the motions between discs. For every line of sight the positions of the clouds are chosen by taking the continuous density distribution to be a probability distribution; i.e. the likelihood of a cloud being at a position in space is proportional to the gas density at that point. Synthetic metal-line profiles are produced taking into account the varying metallicity of the gas in the multiple discs along the sightline as given by the SAMs. The spectrum is smoothed to the resolution of the HIRES spectrograph (Vogt 1992), noise is added and then the four statistics of PW97 are applied. Finally, a Kolmagornov–Smirnoff (KS) test is performed to ascertain the probability that the data of Prochaska & Wolfe (1998) and Wolfe & Prochaska (2000) could be a random subset of the model.

It should be noted that while we try to include all of the relevant physics in the modeling, there are a number of simplifications. The kinematics of sub-halos within the host halos assumes that the sub-halos are on circular orbits and utilizes an approximate formula for the effects of dynamical friction. We assume that the gas discs have a simple radial profile and are axisymmetric. Also we assume that the distribution of the gas does not depend on galaxy environment or Hubble type. We expect that gas discs should be distorted by the presence of other galaxies in the same halo or by previous merger events (cf. McDonald & Miralda-Escudé 1999; Kolatt et al. 1999) yet we ignore these effects. In the spirit of SAMs we hope that these assumptions will capture the essential properties of the resulting DLAS to first order, and we investigate the sensitivity of our results to some of these assumptions. In section 6, we note the good agreement of some of the features of our model with the results of recent hydrodynamical simulations, and in the future we hope to refine our modelling by further comparisons with simulations.

4 RESULTS

4.1 Unsuccessful Models: Classical Discs

In this section we investigate several models based on standard theories of the formation of galactic discs. These theories are generically based on the idea of Mestel (1963) that the specific angular momentum of the material that forms the galactic disc is conserved as it cools and condenses. Since this idea was first applied in the classic work of Fall & Efstathiou (1980), many authors have refined this theory by including the effects of the adiabatic contraction of the dark halo, the presence of a bulge, more realistic halo profiles, and disc stability criteria (Blumenthal et al. 1986; van der Kruit 1987; Flores et al. 1993; Dalcanton, Spergel & Summers 1997; Mo, Mao, & White 1998; van den Bosch 1999).

In the simplest of such models, we assume a singular isothermal profile for the dark matter halo, neglect the effects of the halo contraction on the assembly of the disc, and assume that the profile of the cold gas after collapse has the form of an exponential. The exponential scale length is then given by the simple expression:

$$R_s = \frac{1}{\sqrt{2}}\lambda_H r_i \tag{7}$$

where λ_H is the dimensionless spin parameter of the halo, and r_i is the initial radius of the gas before collapse. In N-body simulations, the spin parameter λ_H for dark matter halos is found to have a log-normal distribution with a mean of about 0.05 (Warren et al. 1992). A generalization of this model, using an NFW profile for the dark matter halo and including the effect of halo contraction, has recently been presented by Mo et al. (1998).

In model EXP1, we assume $\lambda_H = 0.05$ for all halos, take $r_i = \min[r_{cool}, r_{vir}]$, and calculate the scale length for each disc from eqn 7. Note that when this approach is used to model *stellar* scale lengths, the values that we obtain are in good agreement with observations at redshift zero and redshift ~ 3 (SP; SPF).

However local observations (Broeils & Rhee 1997) find that in gas rich galaxies the HI disc always has a larger extent than the stellar disc. To explore this scenario we try a model where the exponential scale length of the gas is given by a multiple of the stellar disc scale length. We find multiplying the scale length calculated from eqn. 7 by a factor of six (model EXP6) produces the best agreement with the kinematic data but can still be rejected at $> 95\%$ confidence level.

In model MMW, we use the fitting formulae of Mo et al. (1998) to obtain the scale radius. In this model we do not use the gas content predicted by the SAMs, but instead, following Mo et al. (1998) we assume that the disc mass is a fixed fraction (one tenth) of the total mass of each halo or sub-halo. This procedure produces roughly three times more cold gas per halo than the SAMs as there is no star-formation and no hot gas. Thus this model should be seen as an upper limit on the amount of cold gas that is available to form DLAS in the halo mass range we are considering. The spin parameter λ_H is chosen randomly from a log-normal distribution, and the exponential scale length is found from eqn 7. The main difference between our MMW model and the actual model of Mo et al. is that we include sub-halos (multiple galaxies in each halo). Because Mo et al. do not

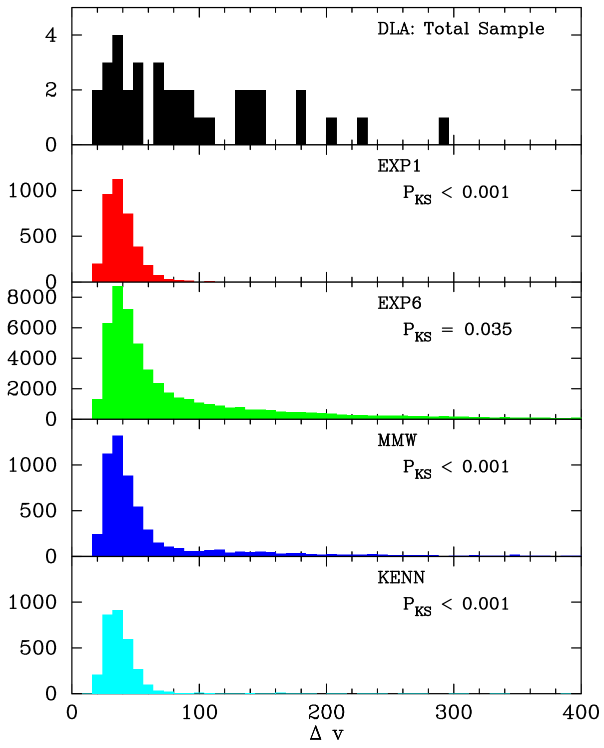

Figure 1. The distribution of the Δv statistic from the data set of Prochaska & Wolfe (1998) and Wolfe & Prochaska (2000) compared to DLAS produced in the four models of section 4.1.

simulate the merging history of their halos, they assume that only one galaxy inhabits each halo (which would correspond to our central galaxy).

The models of K96 used the assumption that the initial profile of the cold gas resulted from conservation of angular momentum, and modelled star formation according to the empirical law proposed by Kennicutt (1989). Kauffmann then found that surface density of the gas discs tended to remain close to the critical surface density, as Kennicutt in fact observed. In our model KENN, based on these observations and the results of K96, we again take the total mass of cold gas from the SAMs, and distribute it at the critical density, which for a flat rotation curve is given by :

$$N_{cr} = 1.5 \times 10^{21}\,\mathrm{cm}^{-2} \left(\frac{V_c}{200\,\mathrm{km\,s}^{-1}}\right)\left(\frac{1\,\mathrm{kpc}}{R}\right). \qquad (8)$$

Thus for a given V_c this is a Mestel distribution, with N_t determined by the above equation and the total mass of cold gas.

The KS test results for the four statistics of PW97 for these four models are shown in Table 1. The most important failing of the models is in the Δv statistic. Fig. 1 shows the distribution of Δv for the data and models. The Δv values produced by these models are peaked around 50 $\mathrm{km\,s}^{-1}$ with very few systems having $\Delta v > 100\,\mathrm{km\,s}^{-1}$, in sharp contrast to the data. This is the same result found in PW97 for a single-disc CDM model (e.g. the model of K96). It is not surprising, as it turns out that in these models most DLAS are in fact produced by a single disc, as shown in Fig. 2. Only for the EXP6 model are half of the DLAS the result of intersections with more than a single gas disc, and only this model has a Δv distribution that is not rejected at greater than 99.9% confidence.

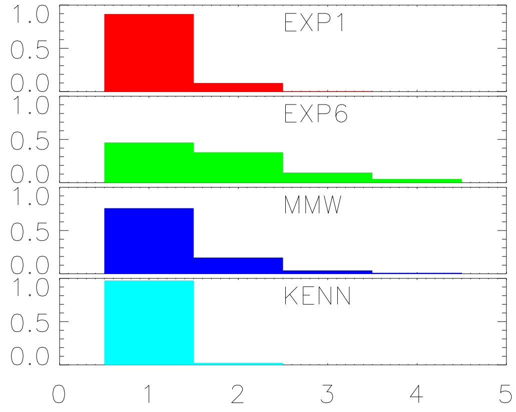

Figure 2. Probability distribution of the number of gaseous discs intersected by a line of sight producing one DLAS. Most of the DLAS are produced by lines of sight passing through a single disc.

Model	Δv	f_{mm}	f_{2pk}	f_{edg}
EXP1	< 0.001	0.006	< 0.001	< 0.001
EXP6	0.035	0.67	0.31	0.16
MMW	< 0.001	0.32	0.026	0.005
KENN	< 0.001	0.005	< .001	.001

Table 1. KS probabilities that the distribution of the four statistics of PW97 for the observed velocity profiles could have been drawn from each of the four models of section 4.1. All of these models can be excluded at high confidence levels.

It is easy to understand why there are so few multiple intersections in these models by examining Fig. 3. This figure shows a projection of the gas discs residing within a halo of circular velocity 156 $\mathrm{km\,s}^{-1}$. The sizes of gas discs in these models are much smaller than the separation between them and thus multiple intersections are rare. The sizes of the gas discs in EXP1 and the KENN model are rather similar. The gas discs in the MMW model are generally bigger because there is more cold gas in each disc and the log-normally distibuted λ_H varies this compared to the EXP1 and KENN models. In these three models almost all the gas is above the column density limit to be considered a damped system. In EXP6 with more extended lower density discs we find some discs where a large fraction of their area lies below the damped level. More extended exponential discs than those considered here do not increase the number of DLAS coming from multiple intersections because the area dense enough to be above the damped limit rapidly shrinks.

In Fig. 4 we show the column density distribution $f(N)$ for these models in comparison with the data of Storrie-Lombardi & Wolfe (2000). Once again, of the four models only EXP6 comes close to fitting the data. Thus although the *total* mass of cold gas is in agreement with that derived from the observations, the total *cross-section* for damped ab-

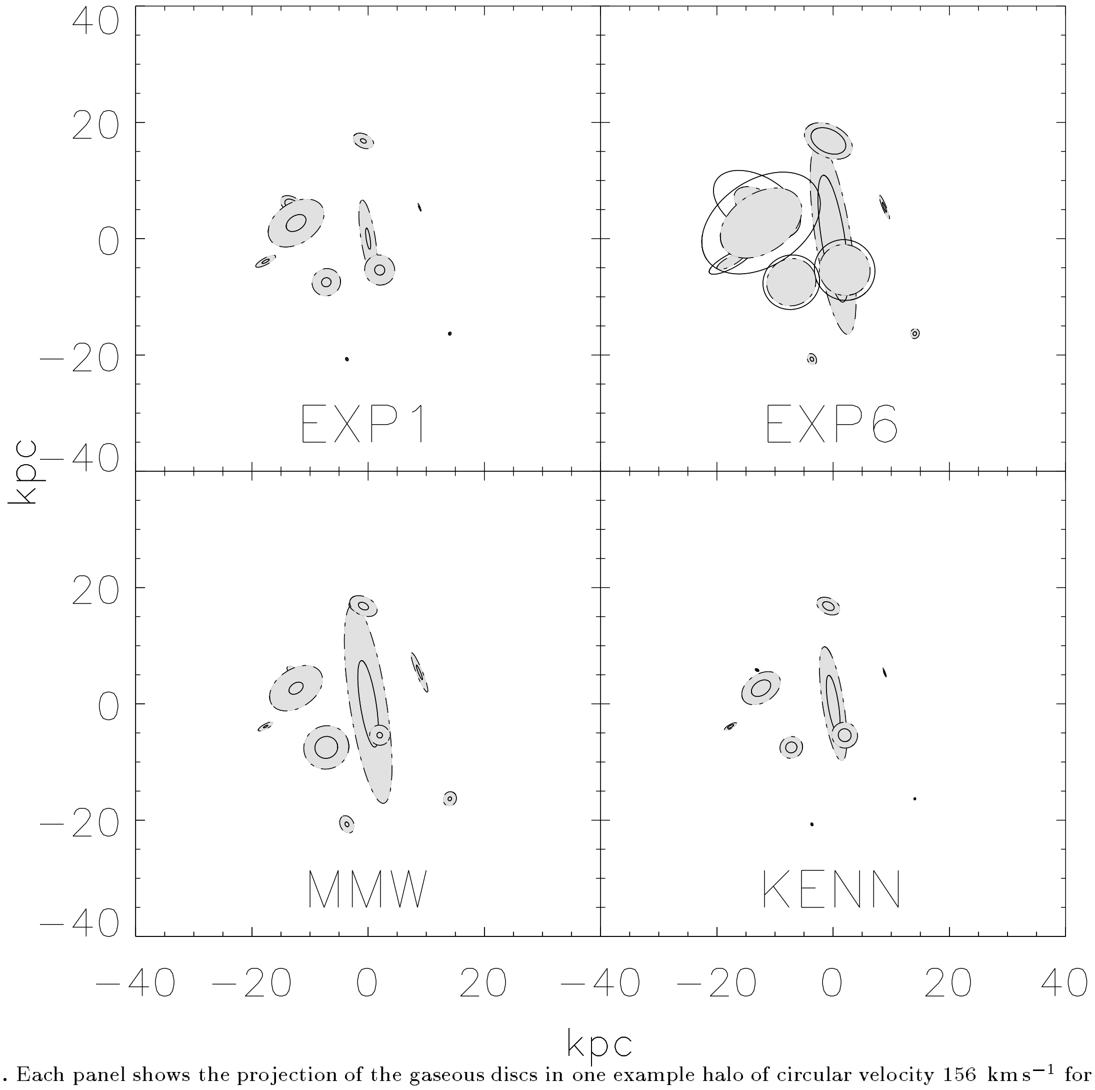

Figure 3. Each panel shows the projection of the gaseous discs in one example halo of circular velocity 156 km s^{-1} for one of the four models of section 4.1. The shaded region is the area of the disc with a column density in excess of 2×10^{20}. The solid line is the half mass radius of the gas disc. One can see that in all these models except for EXP6, a line of sight is unlikely to pass through more than one gaseous disc.

sorption is too small if the gas and stars have a similar radial extent and distribution, as predicted by standard models of disc formation. We therefore conclude that we may need to consider a radically different picture of gaseous discs at high redshift.

$\log(N_t)$	Δv	f_{mm}	f_{2pk}	f_{edg}
19.3	0.04	0.01	0.14	0.27
19.5	0.29	0.03	0.33	0.41
19.6	0.58	0.11	0.68	0.58
19.7	0.18	0.29	0.53	0.73

Table 2. KS probabilities for Mestel discs truncated at a column density N_t.

4.2 Successful Models: Gas Discs with Large Radial Extent

In the previous section we found that models in which the sizes of gas discs at high redshift were calculated from angular momentum conservation fail to reproduce the kinematics and column density distribution of observed DLAS. A model based on the observations of Kennicutt (1989) for local gas discs and the results of the model of K96 also failed. We noted that a common feature of these models is that the majority of DLAS arise from a single galactic disc because of the small radial extent of these discs compared to their separation. If we wish to investigate a scenario like the one proposed by Haehnelt et al. (1998), in which the kinematics of DLAS arise from lines of sight intersecting multiple objects, it is clear that the gaseous discs must be much larger in radial extent.

Unfortunately there does not exist an alternative theoretical framework for the sizes of gas discs, especially at high redshift, so in this section we will simply develop a toy model for the distribution of cold gas. We hope that the insight gained from such a toy model will lead to a more physically motivated model in the future. In our toy models we assume a Mestel profile and assume that the HI discs

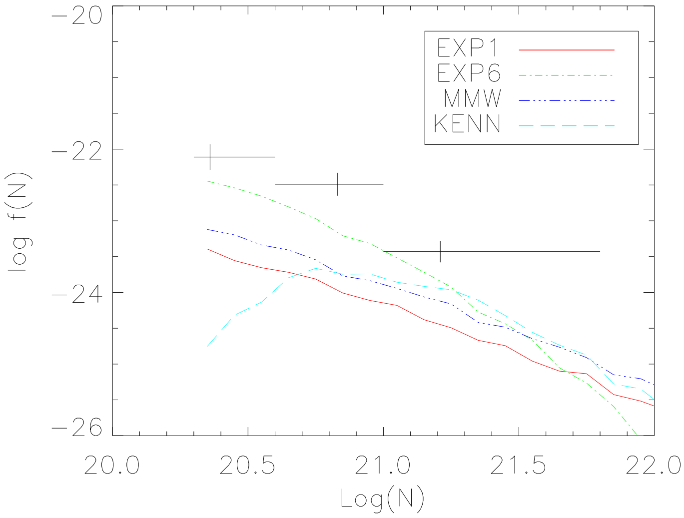

Figure 4. The distribution of column densities, $\log f(N)$ versus $\log(N)$ for the four models of section 4.1 and the data (crosses). Only the EXP6 model comes close to fitting the data. The other three models produce too few DLAS, at least in the ΛCDM cosmology we are considering. The KENN model turns over at low column densities because $\log(N_t)$ is often greater than 20.3 (i.e. we "run out" of gas before reaching the cutoff column density defining a DLAS).

are truncated at a fixed column density, perhaps by a cosmic ionizing background. We investigate a range of values for this critical column density N_t, which is the only additional free parameter of the model. We take the vertical scale height of the gas to be half the *stellar* disc scale length, as calculated from eqn. 7. Since the radial extent of the gas is now so large compared to the stars, this still results in gaseous discs that are quite "thin". We find that our results are only modestly dependent on the assumed vertical scale height, as we show in section 5 (see also Maller et al. 2000b).

The distribution of Δv for several values of N_t between 2 and 5 $\times 10^{19}$ cm^{-2} are shown in Fig. 5. We find that a value for the truncation column density N_t of 4×10^{19} cm^{-2} (i.e., $\log N_t = 19.6$) gives the best fit to the kinematic data. The distribution now shows a significant tail to large values of Δv, in much better agreement with the data. For values of N_t less than 4×10^{19} cm^{-2} the models produce more large values of Δv than are seen in the data, while higher values of N_t produce fewer large values of Δv. Fig. 6 shows the relationship between the number of gaseous discs that produce a DLAS and the truncation level N_t. We see that when $\sim$ 40 percent of the DLAS come from a single gas disc we get the best fit to the kinematic data.

Table 2 shows the KS probabilities for the four statistics of PW97. The mean-median statistic (f_{mm}) shows a clear trend with N_t, such that the statistic improves for higher values of N_t. This is because multiple intersections can produce values of f_{mm} between 0.8 and 1, which are not found in the data. These high values occur in velocity profiles of two narrow peaks separated by a large "valley". An example of this type of profile is the fourth system in Fig. 7. While the statistics of PW97 show agreement between this model and the data, the profiles with $\Delta v > 100$ km/s, whose kinematics are dominated by the motions of the multiple discs relative to one another, show large parts of velocity space

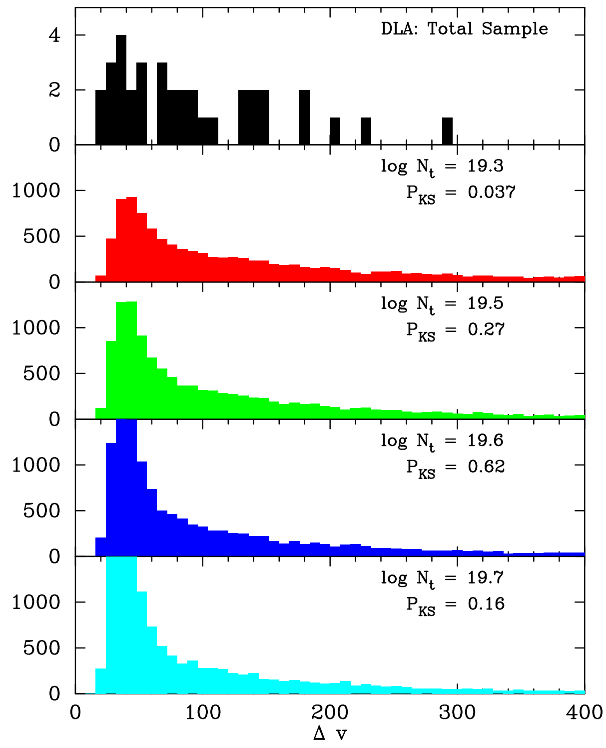

Figure 5. The distribution of Δv for the data and four models where the gas is truncated at a value of $\log N_t = 19.3, 19.5, 19.6, 19.7$. The lower the value of N_t, the larger the radial extent of the gas discs, and therefore the greater the fraction of DLAS that arise from multiple intersections. Multiple intersections tend to create DLAS with large Δv.

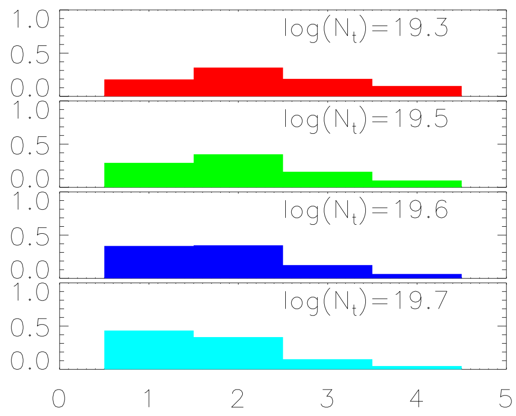

Figure 6. The distribution of the number of gas discs that produce a DLAS for four values of N_t. The distribution of Δv is principally determined by the fraction of DLAS that are produced by "multiple hits" (lines of sight that pass through more than one disc). In this class of models, the best fit to the kinematic data occurs if $\sim$ 40 percent of DLAS come from single discs.

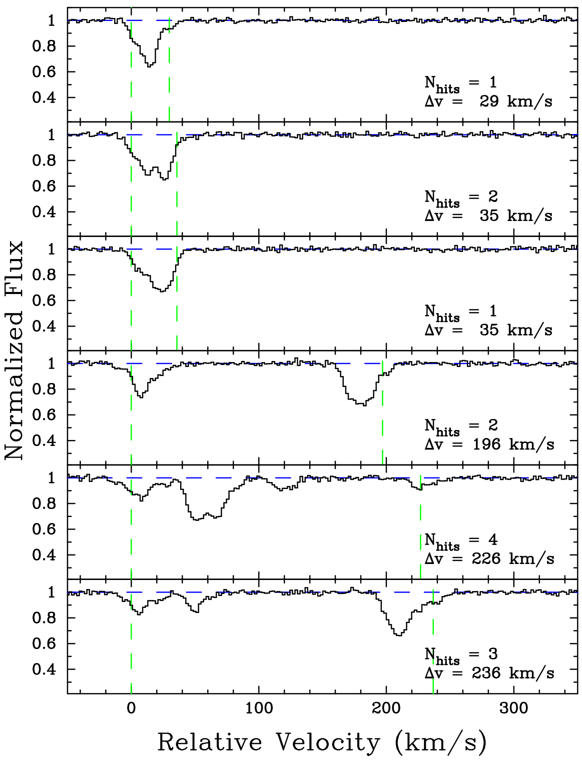

Figure 7. Some examples of the velocity profiles of the low ions in DLAS produced by our modeling in Section 4.2. The dashed line denotes the velocity width Δv of the profile. The profiles with $\Delta v > 100\,\mathrm{km\,s^{-1}}$ have large parts of velocity space with no absorbtion, something not seen in the data. It is possible that this is an artifact of the simplicity of our modeling.

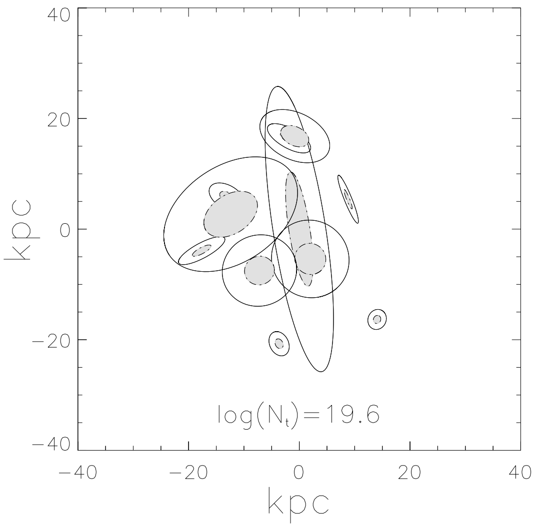

Figure 8. The projection of the gaseous discs in one example halo of circular velocity 156 $\mathrm{km\,s^{-1}}$ for the $N_t = 4 \times 10^{19}\,\mathrm{cm^{-2}}$ model. The shaded region is the area of the disc with a column density in excess of 2×10^{20} and the solid line is the half mass radius of the gaseous disc. One clearly sees that this model will give rise to many lines of sight with multiple intersections.

with no absorbtion (Fig. 7). This is something which is not seen in the data. It is possible that such profiles arise because of the simplicity of our modeling and that in a more physical scenario this configuration would not occur.

The gas discs have such a large radial extent in this model (see Fig. 8) that they will clearly be perturbed by one another and not retain the simple circular symmetry that we are imposing. Perhaps a model in which most of the gas is in tidal streams would be more appropriate. Or perhaps the cold gas is not associated with the individual galaxies at all, but then we must understand what keeps it from being ionized by the extra-galactic UV background. Our toy model demonstrates that the cold gas must somehow be distributed with a very large covering factor in order to reproduce the observed kinematics of the DLAS; understanding how it attains this distribution will require furthur study and most likely hydro simulations.

We now investigate the column density distribution $f(N)$ and the metal abundances for these models. Fig. 9 shows $f(N)$ for the models and the data. The column density distribution is not very sensitive to the truncation density N_t, and all the models produce about the right number of absorbers except in the highest column density bin. This may be due to our simplistic assumption that all gas discs are truncated at the same column density. If a small fraction of them were much denser it might be possible to have enough high column density systems without significantly affecting the kinematic properties of the absorbers. It should also be noted that the data was tabulated assuming a $q_0 = 0$ cosmology, which may introduce an additional discrepancy in comparing to our $q_0 = -0.55$ ΛCDM cosmology. We note that the shape of the distribution is fairly similar to that of the data.

We also show the average metal abundances of our absorbers versus HI column density in Fig. 10. The observational data points are [Zn/H] measurements of DLAS with $z > 2$ (Pettini et al. 1997; Prochaska & Wolfe 1999). One can see our model gives DLAS with metallicities in agreement with the data, and also reproduces the observed trend with HI column density. One might expect that systems with higher HI column densities should have higher metallicities because they are more likely to be in more massive halos. However, because we truncate all gas discs at the same value of N_t the distribution of column densities is the same for all halos masses. Thus our parameterization naturally explains the flat distribution of metal abundances with HI column densities.

5 MODEL DEPENDENCIES

We have presented a model that can produce the observed kinematic properties of the DLAS as well as the other known properties of these systems. In this section we examine the sensitivity of our model to some of the simplifying assumptions we have made. We examine the effect of changing the disc thickness, the orbits of the satellites, the cosmological model, and the assumption of rotationally supported discs. We find that none of these have a large effect on the kinematics of the DLAS in our models. Table 3 shows the KS probabilities when these various assumptions are changed. The effect of any of these changes is less than changing the

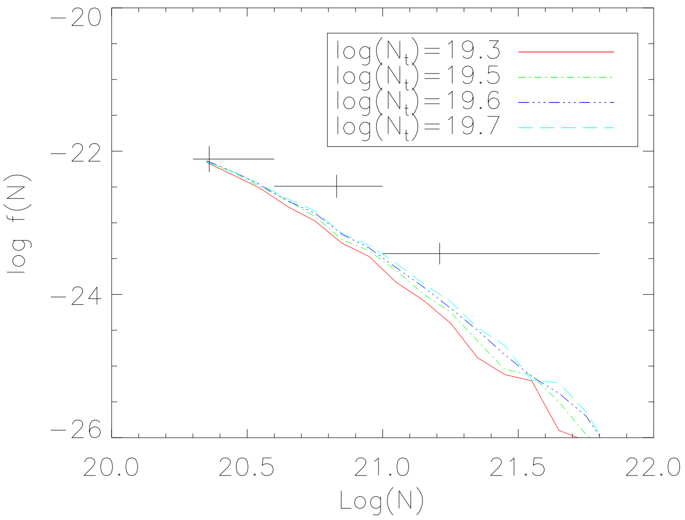

Figure 9. The differential density distribution, $f(N)$ of damped absorbers from the models (lines) compared to the data of Storrie-Lombardi & Wolfe (2000) (crosses). These models fit the two lower column density bins well, but falls short of the highest column density bin.

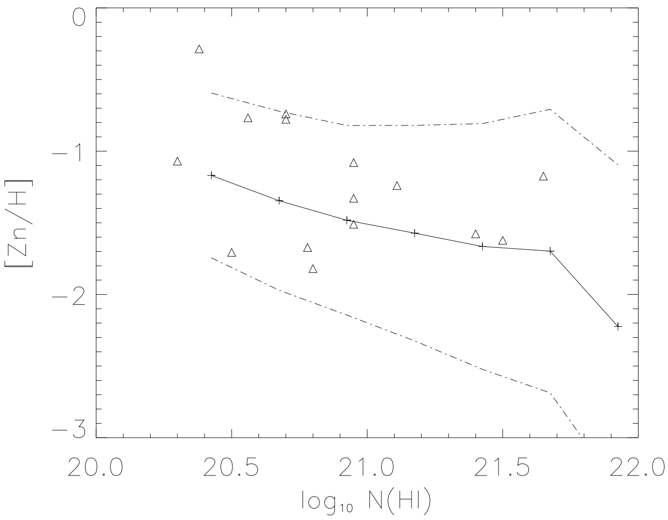

Figure 10. Log(Zn/H) compared to the solar value versus HI column density. The solid line is the average value from our best-fit model and the dot-dash line shows the one sigma spread. The data (triangles) is from Pettini et al. (1997); Prochaska & Wolfe (1999). The spread and trend with column density of the data are consistent with that of our model.

truncation density from $N_t = 4\times10^{19}$ cm^{-2} to 5×10^{19} cm^{-2}. We conclude that our general conclusions are not sensitive to any of these assumptions.

5.1 Disc Thickness

In section 4.2 we assumed the vertical scale length of the gas to be one half the *stellar* disc scale length. Because the gas is so much more radially extended than the stars, this still resulted in very thin discs. One might think that as long as h_z is small compared to the radial size of the discs its exact value would not be important. However, as explained in Maller et al. (2000b) very thin discs have an increased cross section to being nearly edge-on, which changes their kinematic properties. Thus the KS probabilities change non-trivially when we consider thinner discs with $h_z = 0.1R_*$. We favour the model with $h_z = 0.5R_*$ because these large discs are very likely to be warped by interactions, and Prochaska & Wolfe (1998) have shown that using a larger scale height has an effect similar to including warps in the discs. Increasing the disc thickness to $h_z = R_*$ also has a non-negligible effect on the kinematics because thicker discs create a larger Δv for a single disc encounter. Thus there is a trade-off, and we see that we can reproduce the kinematics either with thinner discs with larger radial extent, or thicker discs with smaller radial extent.

5.2 Circular Orbits

We have assumed that all the satellites are on circular orbits within the halo, which is clearly unrealistic. To test the importance of this assumption we explore the opposite extreme, which is to assume that all satellites are on radial orbits. The potential of a SIS is $\Phi(r) = V_c^2 \ln(r)$ so conservation of energy gives us

$$v(r) = \sqrt{2}V_c\sqrt{\ln r_m/r} \tag{9}$$

where r_m is the maximum radius the satellite reaches. From this one can compute that the time it takes for a satellite to travel from r_m to r is given by

$$t(r) = \frac{r_m}{\sqrt{2}V_c}\mathrm{erf}(\ln r_m/r). \tag{10}$$

and that the orbital period is $P = 2\sqrt{2\pi}r_m/V_c$. We find that the expression $r(t) = r_m(1 - .75(4t/P))$ for $0 < t < P/4$ is a reasonable fit to the true function (satellites spend less than 5% of their time in the inner fourth of the orbit). We therefore use it to determine the probability distribution of satellites along their radial orbits. From Table 3 we see that assuming all radial orbits slightly improves the statistics of our model and thus considering a true distribution of orbits will probably only increase the agreement between the data and our model, but not enough to rescue any of the unsuccessful models.

5.3 The Initial Infall Radius of Satellites

As explained in section 3.1, when halos merge the satellite galaxies are placed at a distance f_{mrg}, in units of the virial radius, from the centre of the new halo. One might worry that this parameter, by influencing the position of satellite galaxies in the halo, may be crucial to our DLAS modeling. To test this we try a model with f_{mrg} set to 1.0 (instead of the 0.5 as it has been up to now). This requires us to change the free parameters of the SAMs to maintain the normalization of the reference galaxy, as described in SP. The results of this model are shown in Table 3. Doubling this parameter results in only a modest change in the kinematic properties of DLAS. This is because the important factor is the number of galaxies in the inner part of the halo (which will give rise to multiple intersections); satellites that start their infall from farther out still spend a similar amount of time near the central object which explains the modest effect on the kinematic properties.

Model	Δv	f_{mm}	f_{2pk}	f_{edg}
Default Model	0.57	0.13	0.73	0.58
$h_z = 0.1 R_*$	0.22	0.12	0.57	0.34
$h_z = 1 R_*$	0.28	0.10	0.30	0.46
Radial Orbits	0.60	0.29	0.75	0.66
$f_{mrg} = 1$	0.36	0.14	0.61	0.63
ΛCDM.5	0.72	0.10	0.50	0.64
OCDM	0.28	0.12	0.66	0.68
$z = 2$	0.45	0.17	0.61	0.67
Nonrotating Discs	0.35	0.05	0.42	0.34

Table 3. KS probabilities for variations of the fiducial model.

5.4 Cosmology

So far we have only considered models set within the currently favoured ΛCDM.3 cosmology. However, we would like to know how sensitive our results are to the assumed cosmology. We consider two other cosmologies, a flat universe with $\Omega_0 = 0.5$ (ΛCDM.5) and an open universe with $\Omega_0 = 0.3$ (OCDM.3; as in SP). The free parameters must be readjusted for each cosmology as described in SP. The KS probabilities are listed in Table 3. One sees that the effect of changing the cosmological model is not a drastic one. We do not show the results here, but we note that our conclusions concerning the dynamical tests do not change even in a cosmology with very low $\Omega_0 = 0.1$, nor do they change if we assume $\Omega_0 = 1$. The total mass of cold gas as a function of redshift is rather sensitive to cosmology, however the distribution of Δv is almost completely insensitive to cosmology. This is because the distribution of Δv from single hits depends only on the *shape* of the power spectrum, which is very similar on these scales for any CDM model. The contribution from multiple hits is determined by the dependence of the merger rate on halo mass, which again is a weak function of cosmology.

5.5 Non-Rotating Gas

The final assumption we explore is seemingly a key one: that the cold gas is rotationally supported in discs. We consider a simple alternative model where the cold gas has a bulk velocity with the same magnitude as the circular velocity of the halo, but in a random direction. This might represent gas that is dominated by streaming motion or infall rather than rotation. We are still able to reproduce the observed kinematics, because they are dominated by the motions of the various sub-halos not the motions within the discs. Thus the fundamental assumption that cold gas at high redshift is in rotationally supported discs may need to be reconsidered.

6 PROPERTIES OF GASEOUS DISCS IN OUR MODEL

We have demonstrated that the standard theories of disc formation cannot reproduce the observed properties of DLAS, and have proposed a rather unorthodox alternative which succeeds in reproducing these observations. Here we compare our models with observations of local discs and with results from recent hydrodynamical simulations to assess

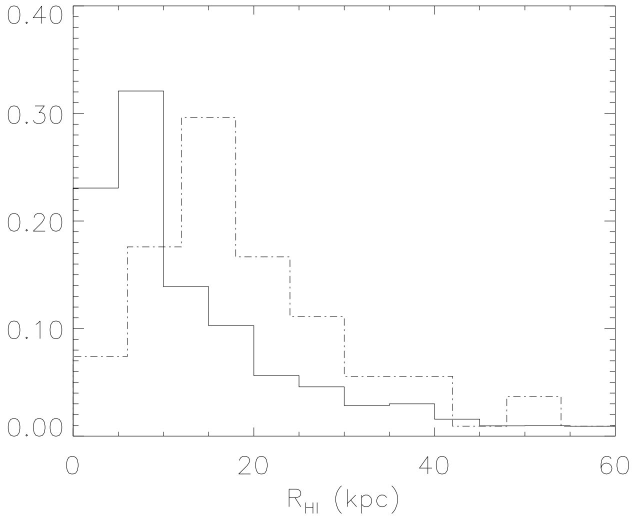

Figure 11. a) The distribution of R_{HI} is plotted for gas discs giving rise to DLAS at $z = 3$ in our fiducial model (solid) and for the data of Broeils & Rhee (1997) (dashed).

whether the model is reasonable. These results are all for the fiducial model of section 4.2.

Because local gas discs do not show a common surface density profile, it is common practice to cite their properties out to some surface density contour, often taken to be 1 $M_\odot \mathrm{pc}^{-2}$ which is equal to $1.25 \times 10^{20}\,\mathrm{cm}^{-2}$. We will denote the radius where the column density reaches this value as R_{HI}. One observed local property of gas discs is that the average surface density $< \sigma_{\mathrm{HI}} >$ out to this level is approximately constant with a value $3.8 \pm 1.1 M_\odot \mathrm{pc}^{-2}$ (Broeils & Rhee 1997). Because in our model all galaxies are normalized by the same value of N_t, the average surface density is identically equal to $2 M_\odot \mathrm{pc}^{-2}$. The galaxies in our model (at $z \sim 3$) thus have an average surface density half the local value and share the property that this value is independent of gas mass.

We can also compare the sizes of gaseous discs in our models to the observations of Broeils & Rhee (1997). Fig. 11 shows the distribution of R_{HI} for the discs that give rise to DLAS in our model (at $z = 3$) and for the local data. The local discs are about twice as large as the high-redshift discs producing the DLAS in our model. The gas discs of the model however extend another factor of 3 before they are truncated, something which is not usually seen locally. Note that as these populations are selected in very different ways, in addition to being at very different redshifts, it is not clear that the distributions should agree closely. However, we see that the radial extent of the gas in our model is not that drastically different from that in local spiral galaxies.

Local HI surveys find no systems with average surface densities less than $5 \times 10^{19}\,\mathrm{cm}^{-2}$ (Zwaan et al. 1997) which is attributed to photo-ionization of HI discs below a column density of a few $10^{19}\,\mathrm{cm}^{-2}$ by the extra-galactic UV background (Corbelli & Salpeter 1993; Maloney 1993). Thus the value of N_t that we attain from considerations of the DLAS kinematics and number density is surprisingly close to local estimates.

If the gas discs in our toy model are truncated because of photo-ionization then we would expect the gas near the truncation edge to have a high ionization fraction. However

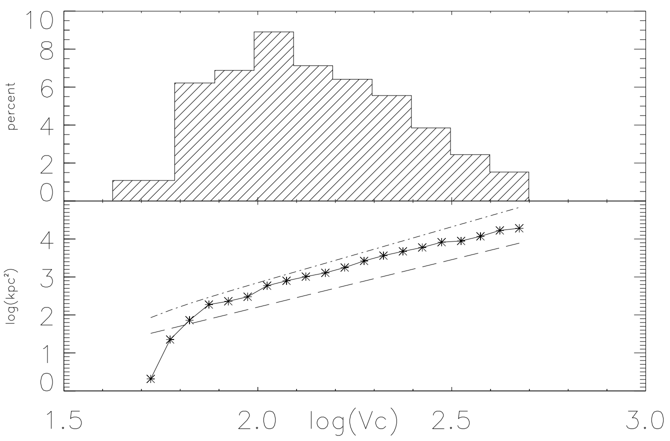

Figure 12. The top panel shows the distribution of circular velocities of the halos that give rise to DLAS in our models. The bottom panel shows the average cross section to damped absorption as a function of circular velocity from our model (solid) and according to Gardner et al. (1997) (dot-dash) and Haehnelt et al. (1999) (dashed). However, Gardner et al. (1999) finds a much shallower slope of 0.9.

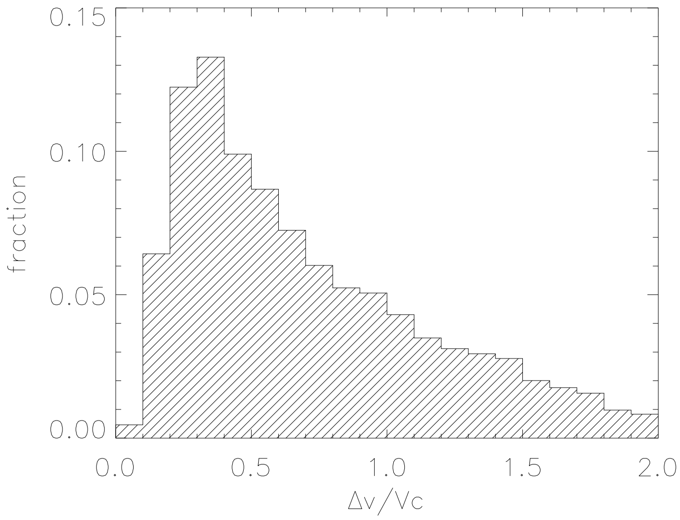

Figure 13. The relationship between the velocity width observed and the circular velocity of the halo in our toy model.

this does not translate into DLAS with high ionization fractions because this low column density gas will only be a fraction of the gas that composes a DLAS. Most of the column density of a DLAS will come from gas at higher densities, as the total needs to be in excess of 2×10^{20} cm^{-2}, and thus the average ionization state of the gas will be low, in agreement with the observations. This model would predict that the lower column density components of the velocity profile would be more likely to have higher ionization states, something that can be checked in the existing data.

It is also interesting to investigate the distribution of halo masses giving rise to DLAS. Fig. 12 shows the distribution of circular velocities of the halos containing discs that give rise to DLAS. Also shown is the average cross section for DLAS as a function of circular velocity, which agrees fairly well with the results of Gardner et al. (1997) (slope = 2.94) and Haehnelt, Steinmetz & Rauch (1999) (slope = 2.5), but not those of Gardner et al. (1999) who finds a much shallower slope of 0.9. Haehnelt et al. determine their average cross section by fitting to the observed Δv distribution so we expect that the relationship between the circular velocity of the halo and the Δv of the DLAS that arise in it must be the same in our modeling and the simulations of Haehnelt et al. . This is in fact the case as can be seen by comparing from Fig. 13 and Fig. 1 in Haehnelt et al. (1999). This seems to suggest that the very different approaches of hydro simulations and SAMs are converging on a common picture for the nature of the DLAS.

7 DISCUSSION AND CONCLUSIONS

We have explored the properties of DLAS in semi-analytic models of galaxy formation. These models produce good agreement with many optical properties of galaxies at low and high redshift, and the total mass of cold gas at redshift ~ 3 is also in reasonable agreement with observations. It is therefore interesting to ask whether the kinematic properties, metallicities, and column densities of DLAS in these models are in agreement with observations. We investigated the dependences of these properties on cosmology, the distribution of satellite orbits, and gaseous disc scale height, and found that our results were not sensitive to these assumptions. Our results are *extremely sensitive* to our assumptions about the radial distribution of cold gas within galactic discs. Given that one believes the other components of our model, one can then perhaps learn about the distribution of cold neutral gas at high redshift.

Currently popular theories of disc formation posit that the radial size of a galactic disc is determined by the initial specific angular momentum of the dark matter halo in which it forms, and that the cold gas traces the stellar component. Often, the profile of the disc is assumed to have an exponential form. We investigate several variants of such models, based on ideas in the literature such as Fall & Efstathiou (1980), Mo et al. (1998) and Kauffmann (1996). We find that the kinematics of DLAS arising in such models are in strong conflict with the observations of Prochaska & Wolfe (1997b, 1998). This is consistent with the previous work of Prochaska & Wolfe, in which it was shown that if the Δv of each DLAS arises from a single rotating disc, generic CDM models can be ruled out at high confidence level. Our work has shown that in theories of disc formation based on angular momentum conservation, the resulting gaseous discs are so small that most DLAS are produced by a single disc and thus the models suffer from the familiar difficulties with the observed kinematics. In addition, although the total mass of cold gas in the models is in agreement with the estimate of Ω_{gas} from Storrie-Lombardi et al. (1996), when we use realistic cross-section-weighted column-density criteria to select DLAS in our models, we find that the overall number density of damped systems is too small. This again seems to indicate that the covering factor of the gas is too small.

We therefore abandon the standard picture of discs and investigate a toy model in which the gas is distributed according to a Mestel distribution with a fixed truncation radius. We adjust the truncation radius as a free parameter to find the best fit with the observations, and find that the best-fit value is consistent with the expected ionization edge due to a cosmic ionizing background. This results in gas discs which are considerably more radially extended than the standard models discussed above. For this class of models, we find good agreement with the four diagnostic statistics of PW97 which describe the kinematics; in particular, the distribution of velocity widths Δv in the models now has a tail to large $\Delta v \sim 200 - 300\,\mathrm{km\,s^{-1}}$ as in the observations. In the models, the majority of these large Δv systems arise from "multiple hits", lines of sight that pass through more than one rotating disc, as in the picture proposed by Haehnelt et al. (1998). The column density distribution and metallicities of the DLAS in the models are also in reasonable agreement with the observations.

This working model for DLAS has many additional implications that may be tested by observations in the near future. One interesting issue is the relationship between DLAS and the Lyman-break galaxies (Steidel et al. 1996; Lowenthal et al. 1997; Steidel et al. 1998), about which little is currently known observationally (Djorgovski 1997; Moller & Warren 1998). Previous theoretical predictions used simplifed relations to estimate luminosities (Mo et al. 1998; Haehnelt et al. 1999). Because the SAMs include detailed modelling of star formation-related processes as well as full stellar population synthesis, we are in a position to make much more detailed and perhaps more reliable predictions. Our model suggests that 20% of DLAS contain at least one galaxy with an R magnitude brighter then 25.5 in the same dark matter halo. The median projected distance between the DLAS and the Lyman-break galaxy is about 30 kpc (Maller et al. 2000a).

Another interesting comparison is with the kinematics of the high ionization state elements (Wolfe & Prochaska 2000). In the simple picture of the SAMs, these profiles would naturally be associated with the gas that has been shock heated to the virial temperature of the halo. The hot gas is distributed spherically in the sub-halo, unlike the cold gas, which would explain why the velocity profiles of the high ions do not trace the low ions (Prochaska & Wolfe 1997a). However, the velocity widths of the two profiles, which are dominated by the motions between sub-halos within the same larger halo, would be related.

The kinematics and $f(N)$ distribution for absorbers below the damped limit but with column densities above the value where the disc is truncated (i.e. Lyman-limit systems) also provide an interesting test of our model. Our modeling suggests that the incidence of these absorbers arising from cold discs should increase with the same slope as in Fig. 9 and then turn over abruptly around a column density of $5 \times 10^{19}\,\mathrm{cm^{-2}}$. Below this column density these Lyman limit systems must be composed of more diffuse ionized gas. This is found in hydro simulations (Davé et al. 1999) and supported by some observational evidence (Prochaska 1999). Thus observations at these column densities can directly probe whether gas discs reach the values of N_t we require to explain the DLAS kinematics and $f(N)$. Lastly it is possible to explore how the properties of the DLAS evolve with redshift. The merging rate is a strong function of redshift (Kolatt et al. 1999, 2000) so we would expect the number of "multiple hits" and therefore the kinematics of the DLAS to be significantly different at low redshift. All these issues will be explored in greater detail in subsequent papers.

If one is really to accept our conclusion that high redshift discs have an extended Mestel-type radial profile, clearly we must develop a theory for their origin. It is possible that the standard theory of disc formation is applicable at low redshift, but that some other process dominates at higher redshift. For example, mergers are far more common at high redshift, and the gas fractions of discs are higher (cf. SPF). This may result in efficient transfer of orbital angular momentum to the gas, producing tidal tails that distribute the gas out to large radii. Locally, some interacting galaxies show extremely extended rotating HI, presumably resulting from such a mechanism (Hibbard 1999). Another possibility is that starbursts triggered by mergers produce supernovae-driven outflows like those seen in local starbursts (Heckman 1999) that could also result in extended gas distributions. We find that a toy model in which the gas clouds have a bulk velocity equal to the rotation velocity of the disc, but in a random direction (i.e. not in a rotationally supported disc) still produces good agreement with the observed DLAS kinematics because the kinematics of our model are dominated by the motions of the multiple discs, not the kinematics within these discs.

It is worth noting that the surface densities of the gas discs in our model would be far below the critical value for star formation determined by observations Kennicutt (1989, 1998), implying that there may be very little star formation taking place in a 'quiescent' mode. It is interesting that SPF found that a picture in which quiescent star formation at high redshift is very inefficient and most of the star formation occurs in merger-induced bursts provides the best explanation of the high redshift Lyman-break galaxies. Even in the extreme case in which quiescent star formation is completely switched off, we find that the starburst mode alone can easily produce the observed level of star formation at high redshift. Thus in the high redshift universe interactions between galaxies seem to play a rather prominent role in determining their gas properties and star formation histories.

ACKNOWLEDGEMENTS

We thank George Blumenthal, James Bullock, Romeel Davé, Avishai Dekel, Martin Haehnelt, Tsafrir Kolatt, Risa Wechsler, and Art Wolfe for stimulating conversations. We thank Lisa Storrie-Lombardi and Art Wolfe for allowing us to use their data prior to publication. This work was supported by NASA and NSF grants at UCSC. AHM and RSS also acknowledge support from University Fellowships from the Hebrew University, Jerusalem and JXP acknowledges support from a Carnegie postdoctoral fellowship. The bibliography was produced with Jonathon Baker's Astronat package.

REFERENCES

Bartelmann M., Loeb A., 1996, ApJ, 457, 529
Blumenthal G. R., Faber S. M., Flores R., Primack J. R., 1986, ApJ, 301, 27
Blumenthal G. R., Faber S. M., Primack J. R., Rees M. J., 1984, Nature, 311, 517
Bosma A., 1981, AJ, 86, 1825
Broeils A. H., Rhee M. H., 1997, A&A, 324, 877

Cole S., Aragon-Salamanca A., Frenk C. S., Navarro J. F., Zepf S. E., 1994, MNRAS, 271, 781
Corbelli E., Salpeter E. E., 1993, ApJ, 419, 104
Dalcanton J. J., Spergel D. N., Summers F. J., 1997, ApJ, 482, 659
Davé R., Hernquist L., Katz N., Weinberg D. H., 1999, ApJ, 511, 521
Djorgovski S. G., 1997, in Structure and Evolution of the Intergalactic Medium from QSO Absorption Line System, Petitjean P., Charlot S., eds., Editions Frontieres, Paris, p. 303
Fall S. M., Efstathiou G., 1980, MNRAS, 193, 189
Flores R., Primack J. R., Blumenthal G. R., Faber S. M., 1993, ApJ, 412, 443
Freeman K. C., 1970, ApJ, 160, 811
Gardner J. P., Katz N., Weinberg D. H., Hernquist L., 1997, ApJ, 486, 42
—, 1999, astro-ph/9911343
Haehnelt M. G., Steinmetz M., Rauch M., 1998, ApJ, 495, 647
—, 1999, astroph/9911447
Heckman T. M., 1999, in After the Dark Ages: When Galaxies were Young, Holt S., Smith E., eds., AIP Press, p. 322
Hibbard J. E., 1999, in Galaxy Dynamics:from the Early Universe to the Present, Combes F., Mamon G. A., Charmandaris V., eds., ASP Conference Series, astroph/9910453
Jedamzik K., Prochaska J. X., 1998, MNRAS, 296, 430
Kauffmann G., 1996, MNRAS, 281, 475
Kauffmann G., Charlot S., 1994, ApJL, 430, L97
Kauffmann G., White S. D. M., Guiderdoni B., 1993, MNRAS, 264, 201
Kennicutt R. C. J., 1989, ApJ, 344, 685
—, 1998, ARA&A, 36, 189
Klypin A., Borgani S., Holtzman J., Primack J., 1995, ApJ, 444, 1
Kolatt T. S., Bullock J. S., Sigad Y., Kravtsov A. V., Klypin A. A., Primack J. R., Dekel A., 2000, in preperation
Kolatt T. S., Bullock J. S., Somerville R. S., Sigad Y., Jonsson P., Kravtsov A. V., Klypin A. A., Primack J. R., et al., 1999, ApJL, 523, L109
Lanzetta K. M., Wolfe A. M., Turnshek D. A., 1995, ApJ, 440, 435
Lowenthal J. D., Koo D. C., Guzman R., Gallego J., Phillips A. C., Faber S. M., Vogt N. P., Illingworth G. D., et al., 1997, ApJ, 481, 673+
Lu L., Sargent W. L. W., Barlow T. A., Churchill C. W., Vogt S. S., 1996, ApJS, 107, 475
Ma C. P., Bertschinger E., 1994, ApJL, 434, L5
Maller A. H., Prochaska J. X., Somerville R. S., Primack J. R., 2000a, in Proceedings of Rencontres Internationales de l'IGRAP, Clustering at High Redshift, Mazure A., Fevre O. L., Brun V. L., eds., AIP Press, in press
Maller A. H., Somerville R. S., Prochaska J. X., Primack J. R., 1999, in After the Dark Ages: When Galaxies were Young, Holt S., Smith E., eds., Vol. 470, AIP Press, p. 102
—, 2000b, in The Hy-Redshift Universe: Galaxy Formation and Evolution at High Redshift, Bunker A., van Breugel W., eds., AIP Press, in press
Maloney P., 1993, ApJ, 414, 41
McDonald P., Miralda-Escudé J., 1999, ApJ, 519, 486
Melchiorri A., Ade P. A. R., de Bernardis P., Bock J. J., Borrill J., et al, 1999, astroph/9911445
Mestel L., 1963, MNRAS, 126, 553
Mo H. J., Mao S., White S. D. M., 1998, MNRAS, 295, 319
Mo H. J., Miralda-Escude J., 1994, ApJL, 430, L25
Moller P., Warren S. J., 1998, MNRAS, 299, 661
Navarro J. F., Frenk C. S., White S. D. M., 1995, MNRAS, 275, 56
Pei Y. C., Fall S. M., 1995, ApJ, 454, 69
Pei Y. C., Fall S. M., Hauser M. G., 1999, ApJ, 522, 604
Perlmutter S., Aldering G., Goldhaber G., Knop R. A., Nugent P., Castro P. G., Deustua S., Fabbro S., et al., 1999, ApJ, 517, 565
Pettini M., Smith L. J., Hunstead R. W., King D. L., 1994, ApJ, 426, 79
Pettini M., Smith L. J., King D. L., Hunstead R. W., 1997, ApJ, 486, 665
Prochaska J. X., 1999, ApJL, 511, L71
Prochaska J. X., Wolfe A. M., 1996, ApJ, 470, 403
—, 1997a, ApJ, 474, 140
—, 1997b, ApJ, 487, 73
—, 1998, ApJ, 507, 113
—, 1999, ApJS, 121, 369
—, 2000, ApJL, submitted
Sheth R. K., Tormen G., 1999, MNRAS, 308, 119
Somerville R. S., 1997, PhD thesis, Univ. California, Santa Cruz
Somerville R. S., Kolatt T. S., 1999, MNRAS, 305, 1
Somerville R. S., Primack J. R., 1999, MNRAS, 310, 1087
Somerville R. S., Primack J. R., Faber S. M., 2000, MNRAS, accepted, astro-ph/9802268
Steidel C. C., Adelberger K. L., Dickinson M., Giavalisco M., Pettini M., Kellogg M., 1998, ApJ, 492, 428
Steidel C. C., Giavalisco M., Pettini M., Dickinson M., Adelberger K. L., 1996, ApJL, 462, L17
Steinmetz M., 1999, in Galaxy Dynamics: from the Early Universe to the Present, Combes F., Mamon G. A., Charmandaris V., eds., ASP Conference Series, p. E24
Storrie-Lombardi L. J., Irwin M. J., MCMahon R. G., 1996, MNRAS, 282, 1330
Storrie-Lombardi L. J., Wolfe A. M., 2000, in preperation
van den Bosch F. C., 1999, astroph/9909298
van der Kruit P. C., 1987, A&A, 173, 59
Vogt S. S., 1992, in ESO Workshop on High Resolution Spectroscopy with the VLT. Editor, M.-H. Ulrich Garching:Germany, p. 223
Warren M. S., Quinn P. J., Salmon J. K., Zurek W. H., 1992, ApJ, 399, 405
White S. D. M., Frenk C. S., 1991, ApJ, 379, 52
White S. D. M., Rees M. J., 1978, MNRAS, 183, 341
Wolfe A. M., 1995, in ASP Conf. Ser. 80: The Physics of the Interstellar Medium and Intergalactic Medium, p. 478
Wolfe A. M., Lanzetta K. M., Foltz C. B., Chaffee F. H., 1995, ApJ, 454, 698
Wolfe A. M., Prochaska J. X., 2000, ApJ, submitted
Wolfe A. M., Turnshek D. A., Smith H. E., Cohen R. D., 1986, ApJS, 61, 249
Zwaan M. A., Briggs F. H., Sprayberry D., Sorar E., 1997, ApJ, 490, 173